

SA-Text: Simple but Accurate Detector for Text of Arbitrary Shapes

Qitong Wang, Yi Zheng, Margrit Betke
 Boston University
 Boston, MA 02215
 {wqt1996, yizheng, betke}@bu.edu

Abstract

We introduce a new framework for text detection named SA-Text meaning “Simple but Accurate,” which utilizes heatmaps to detect text regions in natural scene images effectively. SA-Text detects text that occurs in various fonts, shapes, and orientations in natural scene images with complicated backgrounds. Experiments on three challenging and public scene-text-detection datasets, Total-Text, SCUT-CTW1500, and MSRA-TD500 show the effectiveness and generalization ability of SA-Text in detecting not only multi-lingual oriented straight but also curved text in scripts of multiple languages. To further show the practicality of SA-Text, we combine it with a powerful state-of-the-art text recognition model and thus propose a pipeline-based text spotting system called SAA (“text spotting” is used as the technical term for “detection and recognition of text”). Our experimental results of SAA on the Total-Text dataset show that SAA outperforms four state-of-the-art text spotting frameworks by at least 9 percent points in the F-measure, which means that SA-Text can be used as a complete text detection and recognition system in real applications.

1. Introduction

Scene text detection is an important task in computer vision with application significance such as helping people with visual impairments to understand text in images (e.g., of medicine bottles or supermarket shelves) or helping self-driving cars understand the meaning of traffic and street signs. Building computer vision systems that can detect text is not easy due to the variety of sizes, fonts, styles, sizes, and orientations in which text can occur in natural scene images and their often complex backgrounds.

In the past few years, computer vision researchers have developed methods that identify oriented straight text in natural scene images accurately [14, 26, 43, 45, 46]. More recently, detection of arbitrarily-shaped text, such as curved or deformed text, has received attention from computer vision researchers, not only because detecting such text is



Figure 1. Result visualizations of SA-Text. SA-Text can accurately detect and separate each word in this image relying only on a text region heatmap instead of various kinds of geometric information. Top left: Visualization of the final output of SA-Text. Top right: Heatmap computed by SA-Net. Bottom left: Visualization of the input image with polygonal text annotations. Bottom right: Heatmap of the text region ground truth.

more challenging than oriented straight text, but also because it commonly appears in daily life. For arbitrarily-shaped text detection, for example, a weakly supervised learning algorithm [8] was recently proposed to extract character-based pseudo ground truth to help deep learning models effectively extract each character of such a text in a natural scene image. Whether it is detection of oriented straight or curved text, we found that most state-of-the-art methods rely on multiple deep-learned geometric properties of the text, such as angle attributes [24, 46] or text center line regions [44]. Others use multiple output models [44] to produce high evaluation scores on widely-used bench-

marks. While the state-of-the-art text detection methods can solve many challenging problems with these techniques, as far as we know, there is no method that only uses a “text region feature map” to accurately detect text in natural images. It is very difficult to do this accurately, given the variety of shape, size, and length of text in images. Moreover, many words are located so close to each other in the images that they are not separated correctly but grouped into one consecutive text region. These challenges make relying on only the text region feature map to effectively detect text in natural scene images seemingly impossible. However, is it really impossible to accurately detect text using only one text region feature map in the scene text detection field? The answer is no.

Our proposed methodology clarifies the possibility that outputting only one channel, text region feature map, can also effectively detect text in natural scene images. With the help of new proposed pre-processing and post-processing algorithms, we make it possible that accurately detecting text in images relying on less geometric information of text in natural scene images.

The contributions of our research work are five-fold:

- We propose a new text detection framework, called SA-Text, which outputs only one text region heatmap channel. Not only does SA-Text solve challenging problems in the field of scene text detection, such as accurately detecting and separating multiple text regions that “stick” together, but SA-Text effectively detects small text in natural scene images.
- We propose a new text region feature map representation method, which enables SA-Text to detect text in natural scene image.
- We propose a new post-processing algorithm, Textfill algorithm, which can accurately extract text bounding polygons.
- SA-Text obtained evaluation scores that are higher than most of state-of-the-art scene text detection methods when fine-tuned on specific benchmark datasets. SA-Text outperforms all state-of-the-art methods in its generalization ability, as shown in one of the experiments.
- We introduce a complete pipeline-based text spotting system, showing that our SA-Text can be used in real life as a complete text spotting system if an effective text recognition model is given.

2. Related Works

Scene Text Detection attracts more and more attention from researchers in the computer vision field. In the beginning, researchers mainly focused on detecting oriented straight text in scene images [46, 11, 45, 43, 14]. However, detecting text with arbitrary shapes is more and more popular recently [24, 38, 39, 44, 8, 47, 40].

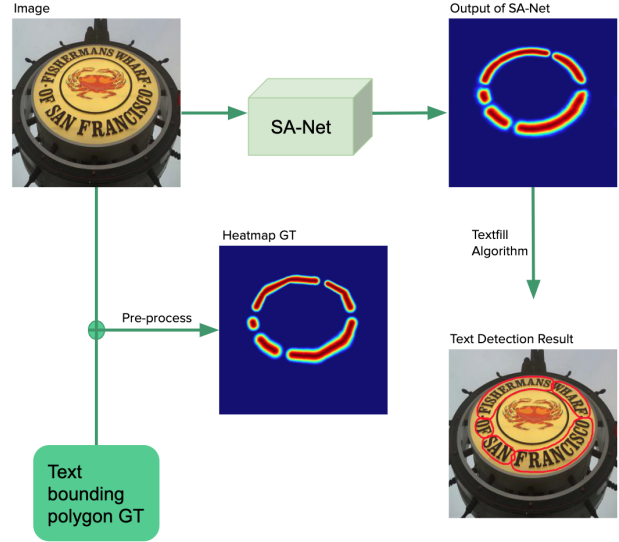


Figure 2. Pipeline of SA-Text. The process of text detection of SA-Text can be divided into three steps: 1) Pre-processing is used to generate a heatmap text region ground truth, which is used as a training label of SA-Net. 2) A trained SA-Net can output predicted text region heatmaps. 3) In the post-processing step, the Textfill algorithm outputs the final predicted text bounding polygons relying on outputs of the SA-Net.

Before methodologies in deep learning field are widely used in text detection field, SWT [12] and MSER [27] were two eye-catching algorithms which had influenced many text detection methodologies. In recent years, modern methodologies, which make use of deep learning backbones, can be coarsely classified into two categories: regression-based methodologies and segmentation-based methodologies.

Regression-based methodologies are largely influenced by some popular general object detection frameworks such as Faster-RCNN [30]. TextBoxes [18] was inspired by SSD [20] and included long default boxes that had large aspect ratios to better detect text with different variation in natural scene images. In the text detection branch of Mask-TextSpotter [25], many text proposals were firstly generated by region proposal network to get text candidate boxes, then the RoI features of the text proposals were sent into the Fast R-CNN module.

Segmentation-based methodologies are mainly inspired by FCN [23], The FCN classifies the image at the pixel level, thus solving the problem of image segmentation at the semantic level. In the text detection field, people see text regions in natural scene images as positive samples and background as negative samples. TextSnake [24] was proposed to detect text in the natural scene by predicting the text region and various geometry attributes of text to detect oriented straight and curve text effectively. Recently,

instead of detecting whole text in images, CRAFT [8] was proposed to detect individual characters, connecting them to get each text bounding polygons. The proposed method provides the character region score and the character affinity score that, together, effectively cover various kinds of text shapes. In this method, a weakly-supervised framework was implemented to generate character-level pseudo annotations.

As we can see, state-of-the-art frameworks make full use of a large volume of geometric information to effectively detect text in natural scene images. But, we will introduce our methodology and run experiments, proving that only using text region information still can effectively extract text bounding polygons from images.

3. Methodology

The pipeline of our model is shown in Figure 2. we will introduce our methodology in details.

3.1. Pre-processing: Heatmap Text Region Ground Truth Generation

Inspired by Textsnake [24], we present each text in images as arbitrary length text skeleton with corresponding text region composing of continuous radius. This representation for text can be flexible enough to present every form of text such as curved or straight.

Heatmap generation is inspired by paper [28, 8]. Instead of simply marking the pixels of the text region as 1, the background pixels as 0, which is like [46, 24], we give a probability to each pixel position in the feature map, indicating the probability that this pixel belonging to the text region. Naturally, the closer the pixel point is to the center of the text, the closer the probability is to 1.0. the farther the pixel point is to the center of the text, the closer the probability is to 0.0. Details are shown in Figure 3.

Getting Text Skeleton and Radius For each text polygon annotation, it consists of an K of points (K is an even number). First, in order to better present each text region, we expand original text annotation points to $m * K$ points ($m \in N^*$). In our experiments, m is set to 5. We then pair the points coordinates of the upper part of the points of polygon with the coordinates of the lower part of the points of polygon. so we have following pairs of point($P_{up}^{(1)}, P_{down}^{(1)}$), ($P_{up}^{(2)}, P_{down}^{(2)}$), ..., ($P_{up}^{(\frac{m*K}{2})}, P_{down}^{(\frac{m*K}{2})}$). For i th pair of points, we could get center point as following:

$$P_{center}^{(i)} = \frac{P_{up}^{(i)} + P_{down}^{(i)}}{2} \quad (1)$$

Then, $P_{center}^{(1)}, P_{center}^{(2)}, \dots, P_{center}^{(\frac{m*K}{2})}$ are defined as **Text Center Points(TCP)**. TCP is essential for building **Text Skeleton(TS)**. In order to get more accurate representation of TS, we need to delete two ends of TCP so the

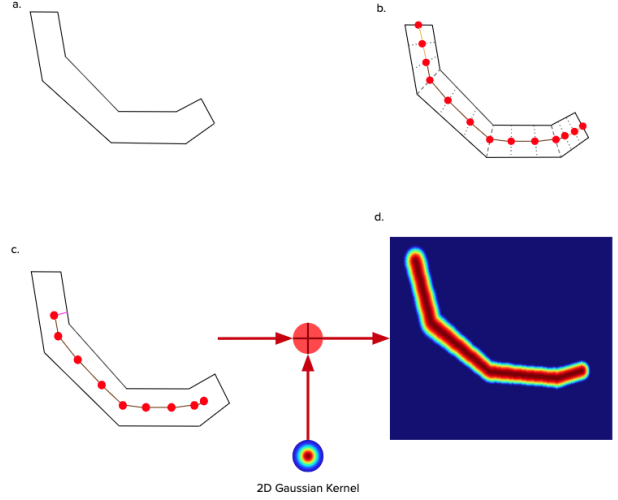


Figure 3. How heatmap ground truth is created. (a) Text bounding polygon annotation. The number of points in this polygon is 10. (b) Text Center Points(TCP) are marked as red dots. To better present each text region, we expand original text annotation points to $m * K$ points. In this figure, $m=3$. Text Skeleton(TS) is drawn as orange and coffee color. (c) In order to get text center region, we delete the two ends of the TS, which is orange line of TS. So we get final TS, which is drawn as coffee color. Definition of R is shown in Equation 2. (d) Final heatmap ground truth. In addition, the range of 2D gaussian kernel is set to $[0.0, 1.0]$ in our methodology.

TCP set are changed from $\{P_{center}^{(1)}, P_{center}^{(2)}, \dots, P_{center}^{(\frac{m*K}{2})}\}$ to $\{P_{center}^{(3)}, P_{center}^{(4)}, \dots, P_{center}^{(\frac{m*K}{2}-2)}\}$. Connecting points in TCP set then we can get TS. For each points in TCP set, we also need their **Radius(R)**. For i th pair of points in Text polygon annotation, $R^{(i)}$ is defined as following:

$$R^{(i)} = \frac{dis(P_{center}^{(i)}, P_{up}^{(i)}) + dis(P_{center}^{(i)}, P_{down}^{(i)})}{2} \quad (2)$$

where function $dis(A, B)$ is the euclidean metric between A and B .

2D Gaussian Heatmap Ground Truth Representation

First we need to get every points of TS using Bresenham [1] algorithm, then we have **All Text Skeleton Points Set (ATSPS)**. Given R set which is $\{R^{(3)}, R^{(4)}, \dots, R^{(\frac{m*K}{2}-2)}\}$ and 2D gaussian kernel, we could get heatmap representation for each text bounding polygon. In addition, the range of generated Heatmap Text Region Ground Truths is set to $[0.0, 1.0]$ in our methodology. These are then used as training labels of SA-Net training.

3.2. SA-Net Architecture and Training Objectives

The backbone of the SA-Net is shown in Figure 4. Inspired by [46, 24, 8], SA-Net is a VGG16-based [33] network that predicts score heatmaps of text regions. First,

images are downsampled to different feature maps. Then these feature maps are gradually upsampled to the original size and mixed with the corresponding output of the previous stage in order to accurately detect text of different sizes.

SA-Net uses an end-to-end training strategy. The definition of the loss function is

$$L = L_{reg} + \lambda_1 L_{center} + \lambda_2 L_{region}, \quad (3)$$

where λ_1 and λ_2 are both set to 1.0.

We define L_{reg} as the weighted MSE-Loss (because the ratio between positive and negative samples is unbalanced in the scene text detection field), which is defined as:

$$L_{reg} = \frac{\sum_{text}}{\sum_{text} + \sum_{BG}} (Y_{BG} - f_{\theta}(\chi_{BG}))^2 + \frac{\sum_{BG}}{\sum_{text} + \sum_{BG}} (Y_{text} - f_{\theta}(\chi_{text}))^2, \quad (4)$$

where *text* means the positive pixels in the heatmap, *BG* means the negative pixels in the heatmap, *Y* means pixels in the generated groundtruth heatmap in pre-process, $f_{\theta}(\chi)$ means pixels in the output of SA-Net, where θ are parameters in SA-Net. The input image is denote by χ .

L_{center} and L_{region} are Dice-Loss [35] for *text*, *center*, and *text region*, respectively. *Text center* is defined as the text region pixels in the output of SA-Net and generated ground truth heatmap pixels which are higher than 0.9. *Text region* is defined as the text region pixels in the output of SA-Net and generated ground truth heatmap pixels which are higher than 0.05, which are:

$$L_{center} = 1 - \frac{2|f_{\theta}(\chi_{center}) \cap Y_{center}|}{|f_{\theta}(\chi_{center})| + |Y_{center}|}, \quad (5)$$

$$L_{region} = 1 - \frac{2|f_{\theta}(\chi_{region}) \cap Y_{region}|}{|f_{\theta}(\chi_{region})| + |Y_{region}|}. \quad (6)$$

3.3. Post-processing: Textfill Algorithm

Extracting the final predicted text bounding polygon from the output of SA-Net is accomplished by our novel post-processing method, the Textfill Algorithm, which is inspired by the floodfill algorithm [2]. Details are show in Algorithm 1, which uses computer vision tools that can be found in OpenCV.

In our proposed Textfill Algorithm, the function $judgeFlow(x_1, y_1, x_2, y_2)$ return true if $I[x_1][y_1] \leq I[x_2][y_2]$ and $I[x_1][y_1] > T_{end}$, or return true if $I[x_1][y_1] \geq T_{end}/2$; function $contourExpand$ is dilating process in morphology tools of OpenCV framework. The kernel of dilating process is defined as:

$$k = \begin{cases} 8 + \frac{S}{750} & S \in (0, 2 * 10^4) \\ 35 & S > 2 * 10^4 \end{cases}$$

where S id the pixel area of text region in each A . Definition of A is given in Algorithm 1.

Algorithm 1 Textfill Algorithm

```

1: Input: Output heatmap from SA-Net,  $I$  ; Threshold:  $T_{top}, T_{end}$ 
2: // Extracting center points for each text region
3: Getting regions where value bigger than  $T_{top}$  in  $I$  are set to 1.0, otherwise are set to 0.0. These regions are defined as  $CR$ 
4: Find center points for each  $CR$ , defined as  $CP$ 
5: // Extracting text region
6:  $L = []$ 
7: for each  $CP$  do
8:   Initializing a zero-like canvas whose shape is as same as  $I$ , defined as  $A$ .
9:    $stack = \text{set}(A[x][y])$ .
10:  while  $stack$  do
11:     $x, y = \text{stack.pop}()$ 
12:    if  $judgeFlow(x-1, y, x, y)$  then
13:       $stack.add((x-1, y))$ 
14:    end if
15:    if  $judgeFlow(x+1, y, x, y)$  then
16:       $stack.add((x+1, y))$ 
17:    end if
18:    if  $judgeFlow(x, y-1, x, y)$  then
19:       $stack.add((x, y-1))$ 
20:    end if
21:    if  $judgeFlow(x, y+1, x, y)$  then
22:       $stack.add((x, y+1))$ 
23:    end if
24:  end while
25:   $A[stack] = 1.0$ 
26:   $C = findCoutour(A)$ 
27:   $L.append(contourExpand(C))$ 
28: end for
29: Output:  $L$ 

```

4. Experiments

In this section, we introduce details of our experiments, including the datasets we use and our training strategy, and provide experimental results and their analysis.

4.1. Text Detection Datasets Used in Experiments

SynthText [13] is a large scale dataset with 800k synthetic images that are created by adding English oriented straight text with random fonts, sizes, colors, and orientations to natural images. These synthetic images are quite similar to natural scene images with text.

Total-Text [9] is a dataset with images that contain oriented straight and curved text and whose labels are annotated by bounding polygons. The image backgrounds are quite similar to real scenes. This dataset contains 1,255 training and 300 testing images.

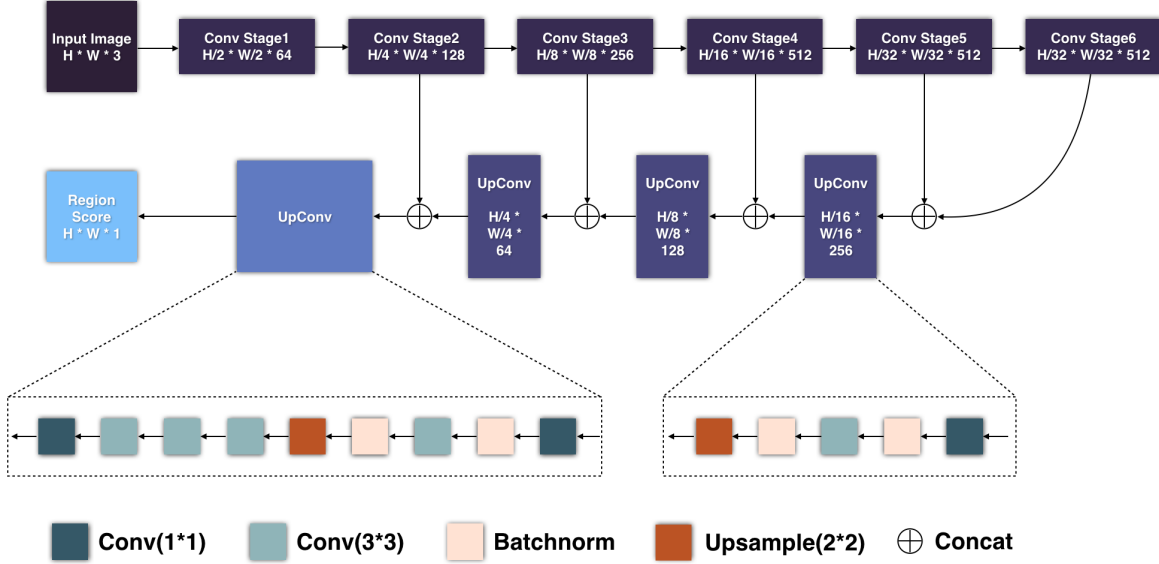


Figure 4. SA-Net Architecture. Conv Stage1 to Conv Stage6 is the pretrained VGG16-based backbone, which is widely used in state-of-the-art scene text detection models [24, 8]

SCUT-CTW1500 [21] is another text detection dataset which includes both English and Chinese scripts. SCTU-CTW1500 contains 1,000 training and 500 testing images in which text is arbitrary like the Total-Text dataset. Text annotations are marked as polygons containing 14 points.

MSRA-TD500 [42] focuses on multi-lingual oriented straight text in natural scenes. It contains 500 images with English and Chinese scripts, which are split into 300 training and 200 testing images. Text region annotations are marked as rotated rectangles.

4.2. Implementation Details

Data Augmentation. The process of training SA-Net can be divided into two steps: 1) Pretraining with the SynthText dataset, and 2) fine-tuning using the Total-Text, SCUT-CTW1500, or MSRA-TD500 datasets respectively. To further improve training, we randomly rotated the training images and cropped with areas ranging from 0.24 to 1.0 and aspect ratios ranging from 0.33 to 3. Data augmentation is implemented in both pretraining and fine-tuning processes.

Training Strategy of SA-Net. Our methodology is implemented in Pytorch 1.0.1 [29]. SA-Net is pretrained on SynthText with one epoch and then fine-tuned using Total-Text, SCUT-CTW1500, or MSRA-TD500. We adopted the Adam optimizer [17] as the learning rate scheme. In the pretraining process, inspired by paper [34], we set the initial learning rate to $3 * 10^{-5}$ and do not change it during the pretraining process. In the fine-tuning process, we set the initial learning rate to 10^{-4} and the decay rate to 0.8 every 10 epochs. Single-scale training is implemented in training process. In the pretraining and fine-tuning training

processes, we set the batch size to 8 on a single RTX-2080Ti GPU. In the evaluation process, batch size is set to 1 on a single RTX-2080Ti GPU.

Hyperparameters setting of Textfill Algorithm. In order to show general experiment results in different datasets, Two thresholds T_{top} , T_{end} are set to (0.7, 0.2) respectively for both Total-Text and SCUT-CTW1500, (0.75, 0.2) for MSRA-TD500.

4.3. Ablation Studies and Experimental Results

The tool used to evaluate the experiments with SA-Text and to reimplement state-of-the-art models is Deteval [3]. We chose the default thresholds (tp=0.4, tr=0.8). The results of the state-of-the-art models are reported here as they were published in the original papers, unless we explain otherwise.

4.3.1 Results for Curved Text Detection

Our results on the benchmarks Total-Text and SCUT-CTW1500 are given in Table 1 and Table 2, respectively. We found that some state-of-the-art methods [44, 40] included multi-scale testing in their framework. To conduct an ablation study, we ran experiments on curved text detection datasets with single-scale and multi-scale testing (abbreviated as “MS” below) separately. In Table 1 and 2, except baselines [9, 21] of datasets, state-of-the-art frameworks without ⁺ used the same pretraining and fine-tuning data as we do, otherwise were different.

Results on Total-Text Dataset (Table 1). Fine-tuning on Total-Text stops at 300 epochs. During the testing pro-

Methodology	Venue	P (%)	R (%)	F (%)
Single-scale Testing				
Poly-FRCNN-3 [9]	IJDAR-2019	78.0	68.0	73.0
Textsnake [24]	ECCV-2018	82.7	74.5	78.4
CSE+ [22]	CVPR-2019	81.4	79.7	80.2
TextField [41]	TIP-2019	81.2	79.9	80.6
PSENet-1s+ [38]	CVPR-2019	84.02	77.96	80.87
FTSN [10]	ICPR-2018	84.7	78.0	81.3
ICG [37]	PR-2019	82.9	80.9	81.5
LOMO [44]	CVPR-2019	88.6	75.7	81.6
CRAFT+ [8]	CVPR-2019	87.6	79.9	83.6
PSENet_v2 [39]	ICCV-2019	89.3	81.0	85.0
CharNet H-88 [40]	ICCV-2019	89.9	81.7	85.6
SA-Text (Ours)	-	88.8	82.6	85.6
Multi-scale Testing				
LOMO MS [44]	CVPR-2019	87.6	79.3	83.3
CharNet H-88 MS [40]	ICCV-2019	88.0	85.0	86.5
SA-Text MS (Ours)	-	85.0	85.6	85.3

Table 1. Experiment results on the Total-Text Dataset. To ensure fairness and provide an ablation study, we separate the results of single-scale testing from the results of multi-scale testing. “P” means Precision; “R” means Recall; “F” means F-measure. MS denotes multi-scale testing.

cess, each image is set to 700*700. In single-scale testing, our SA-Text beats all of the state-of-the-art methodologies and keeps the same F-measure score with the newest and most competitive model, CharNet H-88 [40]. SA-Text MS even yields a higher recall rate than all the other state-of-the-art methods, 85.6%. This indicates that SA-Text is able to detect text that is missed by other methods.

Results on SCUT-CTW1500 Dataset (Table 2). Fine-tuning on SCUT-CTW1500 stops at 307 epochs. During the testing process, each image is set to 500*500 because the average size of images in SCUT-CTW1500 is relatively smaller than that of Total-Text. Similar to experiments with Total-Text, we conduct a multi-scale ablation study. Experimental results shows that SA-Text also performs well on SCUT-CTW1500. Surprisingly, SA-Text found image text that did not appear in the ground truth annotation (see Figure 5). We fixed the SCUT-CTW1500 ground truth to include missed words. To ensure fairness in evaluation, we ran experiments on two different versions of text annotations on the SCUT-CTW1500 dataset, with and without updated ground truth (Table 2). After the ground truth was updated, the recall score of SA-Text is almost unchanged but the precision score improves a little. We welcome other researchers to run experiments on the updated SCUT-CTW1500 and therefore make it publicly available.

Analysis on Multi-scale Testing. In our multi-scale testing, we tested our model with images of different sizes, relying on Fast NMS algorithm to screen out excess text bounding polygons. A reason for the increase of the recall score of multi-scale compared to single-scale testing may be that multi-scale testing combines image information of different sizes, making it easier for SA-Text to detect text

Methodology	Venue	P (%)	R (%)	H (%)
Single-scale Testing				
CTD [21]	PR-2019	74.3	65.2	69.5
CTD+TLOC [21]	PR-2019	74.3	69.8	73.4
Textsnake [24]	ECCV-2018	67.9	85.3	75.6
CSE+ [22]	CVPR-2019	78.7	76.1	77.4
LOMO [44]	CVPR-2019	89.2	69.6	78.4
ICG [37]	PR-2019	82.8	79.8	81.3
TextField [41]	TIP-2019	83.0	79.8	81.4
CRAFT [8]	CVPR-2019	86.0	81.1	83.5
PSENet_v2 [39]	ICCV-2019	86.4	81.2	83.7
PAN Mask R-CNN+ [15]	WACV-2019	86.8	83.2	85.0
SA-Text (Ours)	-	84.3	84.8	84.5
SA-Text* (Ours)	-	86.2	84.1	85.2
Multi-scale Testing				
LOMO MS [44]	CVPR-2019	85.7	76.5	80.8
SA-Text MS (Ours)	-	83.3	85.4	84.4
SA-Text MS* (Ours)	-	85.2	84.7	85.0

Table 2. Experiment results on SCUT-CTW1500 Dataset. To ensure fairness and the principle of ablation studies, we separate the results of single-scale testing and the results of multi-scale testing. “P” means Precision; “R” means Recall; “H” means H-mean. * denotes experiment results on updated groundtruth annotations that we modified for SCUT-CTW1500. MS denotes multi-scale testing.



Figure 5. Ground truth annotation update. SCUT-CTW1500 ground truth annotation misses “89”(top left) and “©Roberto Herrett” (bottom left). The updated annotations are visualized in the images on the right.

regions that are difficult to detect in single-scale testing. However, false-positive samples are more likely to appear in multi-scale testing. We think that might be caused by the effort of the Fast NMS algorithm or text detection effect on very large images, all of which cause decrease of precision score of multi-scale testing (see Tables 1 and 2).

Methodology	Venue	P (%)	R (%)	H (%)
Zhang et al. [45]	CVPR-2016	83	67	74
He et al. [14]	CVPR-2017	77	70	74
EAST [†] [46]	CVPR-2017	87.3	67.4	76.1
SegLink [31]	CVPR-2017	86	70	77
PixelLink [†] [11]	AAAI-2018	83.0	73.2	77.8
Textsnake [24]	ECCV-2018	83.2	73.9	78.3
RRD [†] [19]	CVPR-2018	87	73	79
Lyu et al. [†] [26]	CVPR-2018	87.6	76.2	81.5
CRAFT [8]	CVPR-2019	88.2	78.2	82.9
SA-Text (Ours)	-	84.2	76.2	80.0

Table 3. Experiment results on MSRA-TD500 Dataset; "P" means Precision; "R" means Recall; "H" means H-mean. [†] denotes results based on multi-scale testing. Note that in this table, training data and testing scale of different methods may not be the same, and thus the comparison is not strictly fair.

Dataset		Total-Text			SCUT-CTW1500		
Methodology	Venue	P (%)	R (%)	F (%)	P (%)	R (%)	H (%)
SegLink [31]	CVPR-2017	35.6	33.2	34.4	33.0	28.4	30.5
EAST [46]	CVPR-2017	49.0	43.1	45.9	46.7	37.2	41.4
PixelLink [11]	AAAI-2018	53.5	52.7	53.1	50.6	42.8	46.4
Textsnake [24]	ECCV-2018	61.5	67.9	64.6	65.4	63.4	64.4
CRAFT [8]	CVPR-2019	63.0	72.9	67.6	64.5	62.0	63.3
CRAFT* [8]	CVPR-2019	-	-	-	65.5	61.3	63.3
SA-Text (Ours)	-	71.3	70.2	70.7	73.1	75.3	74.2
SA-Text* (Ours)	-	-	-	-	74.5	74.7	74.6

Table 4. Experiment results for generalization ability on Total-Text and SCUT-CTW1500 datasets; "P" means Precision; "R" means Recall; "F" means F-measure; "H" means H-mean. Results of Seglink [31], EAST [46], PixelLink [11] and Textsnake [24] are reported on [24]. Results of CRAFT [8] are from official CRAFT model [4] which was fine-tuned on the ICDAR-2015 dataset. * denotes experiment results on updated text annotations that we modified for SCUT-CTW1500. Single-scale testing is implemented when we run this experiment for SA-Text.

4.3.2 Results on Multi-lingual Oriented Straight Text Detection Dataset

We chose MSRA-TD500 dataset as the standard text detection benchmark. Fine-tuning on MSRA-TD500 stops at 200 epochs. During the testing process, each image is set to 512*512. For SA-Text, only single-scale testing is implemented in this experiment. The results (Table 3) show that our SA-Text beats most of the state-of-the-art methods on MSRA-TD500, demonstrating that SA-Text is general and can be readily applied to detecting multi-lingual oriented straight text in natural scenes.

4.3.3 Generalization Ability

A powerful text detection framework should have good generalization ability instead of just overfitting to a particular dataset and reaching high evaluation scores for that dataset. To further verify the generalization ability of SA-Text, we pretrained and fine-tuned our model on datasets without curved text and then evaluated it on the Total-Text and SCUT-CUW1500 datasets. In particular, we fine-tuned our model on ICDAR-2015 [16] dataset with 200 epochs,

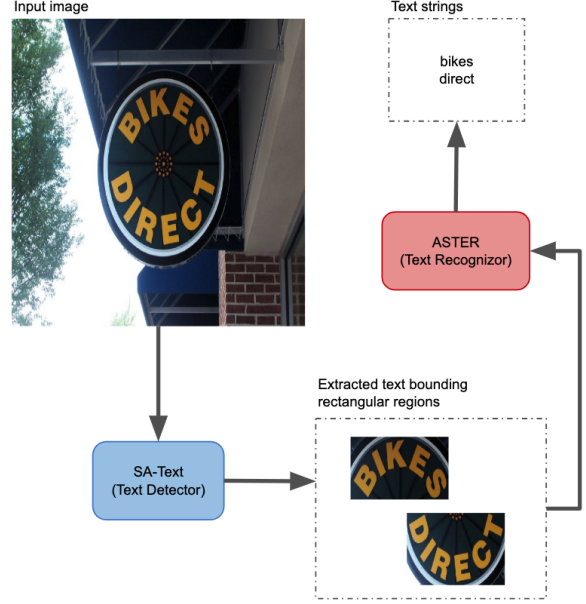


Figure 6. Pipeline of the proposed text spotting model SAA. The model first calls the proposed SA-Text Detector and then converts SA-Text’s polygonal output regions into horizontally-aligned rectangular regions of text. These text regions are then passed to the state-of-the-art text recognition model ASTER [32], which can accurately recognize the text in these regions and outputs text strings.

then evaluated on the two datasets. We choose state-of-the-art baselines which were also only fine-tuned on ICDAR-2015 [16] dataset. Results are shown in Table 4.

Experiment results show that SA-Text still performs well on two challenging datasets even if not fine-tuned on them and even outperforms five effective state-of-the-art baselines. We think the powerful generalization ability of SA-Text is mainly because of the flexibility of text expression and the effective Textfill Algorithm, which can make full use of SA-Net’s output information to effectively extract text bounding polygons.

4.4. Experimental Results on Text Spotting

So far, we have shown that the proposed SA-Text model can accurately localize text in natural scene images. The application range of SA-Text can be widened when it is embedded into a text recognition framework. After all, a sighted person would not stop at the task of localizing text but also aim to identify its content. To provide a computer vision system who can take on both tasks of detecting and recognizing text in images, we here propose the model SAA (short for SA-Text + ASTER [32]) that can “spot” text in images, which means detect and recognize it. The pipeline of SAA is shown in Figure 6. We also present an ablation study for SAA, showing the contribution of SA-Text in accurate text spotting. We built another pipeline-

Methodology	Venue	F-measure (%)
Textboxes [18]	AAAI-2017	36.3
Mask TextSpotter [25]	ECCV-2018	52.9
TextNet [36]	ACCV-2018	54.0
CharNet H-88 [40]	ICCV-2019	66.6
TSA [24, 32]	ECCV-2018	58.1
SAA (Ours) [32]	-	75.7

Table 5. Experiment results of TSA and SAA on the Total-Text Dataset. Pretrained ASTER [32] model is downloaded from official pytorch reimplementation [6]. Evaluation method for SAA and TSA is end-to-end recognition from [7]. Annotations are horizontal text-bounding rectangles because SA-Text and TextSnake outputs horizontal text-bounding rectangles in SAA and TSA. No distinction between uppercase and lowercase was made when we evaluated SAA and TSA. The listed F-measures of the prior works were reported in their original papers.



Figure 7. Sample text spotting result of SAA. Like a person, SAA does not only know where the text regions are, but also recognize the content of each text region.

based text spotting system called **TSA** (TextSnake [24] + ASTER [32]) which applies the pretrained TextSnake model [5] with the same training data as SA-Text.

We ran experiments using the Total-Text dataset, where annotations of text spotting are included. Single-scale and lexicon-free testing are implemented in the evaluation for all models. Experimental results are detailed in Table 5, which show that SAA has a powerful ability to spot text and outperforms state-of-the-art text spotting systems on the Total-Text dataset. Moreover, since the same conditions were applied for SAA and TSA, the superior results of SAA shows the effectiveness of SA-Text as the text detection module of the text spotting pipeline. Because SA-Text accurately localizes text regions, the ASTER module of SAA can be effective in recognizing the text in these regions (see Figure 7).

4.5. Analysis and Discussion

Framework Features SA-Text is robust to different scales and shapes of text from natural scene images. SA-Text treats the text in the natural scene images directly as positive regions instead of the composition of different geometry attributes, whether it is oriented straight text or curved text. Textfill algorithm can also flexibly and accurately extract the text in the images according to the output of SA-Net. Even if the text is very close to each other, SA-Text can accurately separate the text and output accurate final results, outperforming most of the state-of-the-art methodologies in the text detection field.

Multi-lingual Ability SA-Text now can detect English and Chinese scripts in our experiments. SCUT-CTW1500 and MSRA-TD500 contain English and Chinese scripts. Experiment results on SCUT-CTW1500 and MSRA-TD500 show its effectiveness when detecting Latin languages such as English and Sino-Tibetan language like Chinese.

Generalization Ability SA-Text outperforms state-of-the-art text detection framework by 3.1% in the F-measure of Total-Text [9] and at least 10.9% in the F-measure of SCUT-CTW1500 [21] even not fine-tuned on them, which show that SA-Text has powerful generalization ability when comparing with state-of-the-art text detection frameworks for the pioneering learning ability of SA-Net and the simplicity but the effectiveness of Textfill Algorithm. By comparing the experimental results from Table 1 to 3 with that from Table 4, we find that SA-Text performs well when fine-tuned to a specific dataset while having excellent generalization ability, which proves the robustness of SA-Text.

Text Spotting Analysis The excellent experimental results of SAA (Table 5) clarifies the broad application range of our SA-Text. Besides powerful generalization ability, SA-Text also performs excellent if used as a text detector in one pipeline-based text spotting system.

5. Conclusion

In this paper, we proposed a new text detection model called SA-Text that, with little information, can effectively detect text in natural scene images. SA-Text performs well in three experiments with publicly available datasets. This includes experiments with SA-Text when fine-tuned and tested on a specific dataset and when fine-tuned and tested on different datasets. We fixed ground truth annotation errors of the SCUT-CTW1500 dataset and make the corrected ground truth publicly available. We further strengthened the application scope of SA-Text by implementing a pipeline-based text spotting system. In the future, we plan to explore the possibility of detecting scripts of languages other than English and Chinese scripts, such as Korean and Arabic scripts, with SA-Text.

References

- [1] https://en.wikipedia.org/wiki/Bresenham%27s_line_algorithm. 3
- [2] https://en.wikipedia.org/wiki/Flood_fill. 4
- [3] https://github.com/cs-chan/Total-Text-Dataset/tree/master/Evaluation_Protocol. 5
- [4] <https://github.com/clovaai/CRAFT-pytorch>. 7
- [5] <https://github.com/princewang1994/TextSnake.pytorch>. 8
- [6] <https://github.com/ayumiymk/aster.pytorch>. 8
- [7] https://github.com/liuheng92/OCR_EVALUATION. 8
- [8] Y. Baek, B. Lee, D. Han, S. Yun, and H. Lee. Character region awareness for text detection. *CoRR*, abs/1904.01941, 2019. 1, 2, 3, 5, 6, 7
- [9] C. K. Chng and C. S. Chan. Total-text: A comprehensive dataset for scene text detection and recognition. *CoRR*, abs/1710.10400, 2017. 4, 5, 6, 8
- [10] Y. Dai, Z. Huang, Y. Gao, and K. Chen. Fused text segmentation networks for multi-oriented scene text detection. *CoRR*, abs/1709.03272, 2017. 6
- [11] D. Deng, H. Liu, X. Li, and D. Cai. Pixellink: Detecting scene text via instance segmentation. *CoRR*, abs/1801.01315, 2018. 2, 7
- [12] B. Epshtein, E. Ofek, and Y. Wexler. Detecting text in natural scenes with stroke width transform. *2010 IEEE Computer Society Conference on Computer Vision and Pattern Recognition*, pages 2963–2970, 2010. 2
- [13] A. Gupta, A. Vedaldi, and A. Zisserman. Synthetic data for text localisation in natural images. *CoRR*, abs/1604.06646, 2016. 4
- [14] W. He, X. Zhang, F. Yin, and C. Liu. Deep direct regression for multi-oriented scene text detection. *CoRR*, abs/1703.08289, 2017. 1, 2, 7
- [15] Z. Huang, Z. Zhong, L. Sun, and Q. Huo. Mask R-CNN with pyramid attention network for scene text detection. *CoRR*, abs/1811.09058, 2018. 6
- [16] D. Karatzas, L. Gomez-Bigorda, A. Nicolaou, S. Ghosh, A. Bagdanov, M. Iwamura, J. Matas, L. Neumann, V. R. Chandrasekhar, S. Lu, et al. Icdar 2015 competition on robust reading. In *2015 13th International Conference on Document Analysis and Recognition (ICDAR)*, pages 1156–1160. IEEE, 2015. 7
- [17] D. P. Kingma and J. Ba. Adam: A method for stochastic optimization. *arXiv preprint arXiv:1412.6980*, 2014. 5
- [18] M. Liao, B. Shi, X. Bai, X. Wang, and W. Liu. Textboxes: A fast text detector with a single deep neural network. *CoRR*, abs/1611.06779, 2016. 2, 8
- [19] M. Liao, Z. Zhu, B. Shi, G. Xia, and X. Bai. Rotation-sensitive regression for oriented scene text detection. *CoRR*, abs/1803.05265, 2018. 7
- [20] W. Liu, D. Anguelov, D. Erhan, C. Szegedy, S. E. Reed, C. Fu, and A. C. Berg. SSD: single shot multibox detector. *CoRR*, abs/1512.02325, 2015. 2
- [21] Y. Liu, L. Jin, S. Zhang, and S. Zhang. Detecting curve text in the wild: New dataset and new solution. *CoRR*, abs/1712.02170, 2017. 5, 6, 8
- [22] Z. Liu, G. Lin, S. Yang, F. Liu, W. Lin, and W. L. Goh. Towards robust curve text detection with conditional spatial expansion. *CoRR*, abs/1903.08836, 2019. 6
- [23] J. Long, E. Shelhamer, and T. Darrell. Fully convolutional networks for semantic segmentation. *CoRR*, abs/1411.4038, 2014. 2
- [24] S. Long, J. Ruan, W. Zhang, X. He, W. Wu, and C. Yao. Textsnake: A flexible representation for detecting text of arbitrary shapes. In *The European Conference on Computer Vision (ECCV)*, September 2018. 1, 2, 3, 5, 6, 7, 8
- [25] P. Lyu, M. Liao, C. Yao, W. Wu, and X. Bai. Mask textspotter: An end-to-end trainable neural network for spotting text with arbitrary shapes. *CoRR*, abs/1807.02242, 2018. 2, 8
- [26] P. Lyu, C. Yao, W. Wu, S. Yan, and X. Bai. Multi-oriented scene text detection via corner localization and region segmentation. *CoRR*, abs/1802.08948, 2018. 1, 7
- [27] J. Matas, O. Chum, M. Urban, and T. Pajdla. Robust wide-baseline stereo from maximally stable extremal regions. *Image and vision computing*, 22(10):761–767, 2004. 2
- [28] A. Newell, K. Yang, and J. Deng. Stacked hourglass networks for human pose estimation. *CoRR*, abs/1603.06937, 2016. 3
- [29] A. Paszke, S. Gross, S. Chintala, G. Chanan, E. Yang, Z. DeVito, Z. Lin, A. Desmaison, L. Antiga, and A. Lerer. Automatic differentiation in pytorch. 2017. 5
- [30] S. Ren, K. He, R. B. Girshick, and J. Sun. Faster R-CNN: towards real-time object detection with region proposal networks. *CoRR*, abs/1506.01497, 2015. 2
- [31] B. Shi, X. Bai, and S. J. Belongie. Detecting oriented text in natural images by linking segments. *CoRR*, abs/1703.06520, 2017. 7
- [32] B. Shi, M. Yang, X. Wang, P. Lyu, C. Yao, and X. Bai. Aster: An attentional scene text recognizer with flexible rectification. *IEEE transactions on pattern analysis and machine intelligence*, 2018. 7, 8
- [33] K. Simonyan and A. Zisserman. Very deep convolutional networks for large-scale image recognition. *arXiv preprint arXiv:1409.1556*, 2014. 3
- [34] L. N. Smith. No more pesky learning rate guessing games. *CoRR*, abs/1506.01186, 2015. 5
- [35] C. H. Sudre, W. Li, T. Vercauteren, S. Ourselin, and M. J. Cardoso. Generalised dice overlap as a deep learning loss function for highly unbalanced segmentations. *CoRR*, abs/1707.03237, 2017. 4
- [36] Y. Sun, C. Zhang, Z. Huang, J. Liu, J. Han, and E. Ding. Textnet: Irregular text reading from images with an end-to-end trainable network. *CoRR*, abs/1812.09900, 2018. 8
- [37] J. Tang, Z. Yang, Y. Wang, Q. Zheng, Y. Xu, and X. Bai. Detecting dense and arbitrary-shaped scene text by instance-aware component grouping. *Pattern Recognition*, 2019. 6

- [38] W. Wang, E. Xie, X. Li, W. Hou, T. Lu, G. Yu, and S. Shao. Shape robust text detection with progressive scale expansion network. *CoRR*, abs/1903.12473, 2019. 2, 6
- [39] W. Wang, E. Xie, X. Song, Y. Zang, W. Wang, T. Lu, G. Yu, and C. Shen. Efficient and accurate arbitrary-shaped text detection with pixel aggregation network. *arXiv preprint arXiv:1908.05900*, 2019. 2, 6
- [40] L. Xing, Z. Tian, W. Huang, and M. R. Scott. Convolutional character networks. *arXiv preprint arXiv:1910.07954*, 2019. 2, 5, 6, 8
- [41] Y. Xu, Y. Wang, W. Zhou, Y. Wang, Z. Yang, and X. Bai. Textfield: Learning A deep direction field for irregular scene text detection. *CoRR*, abs/1812.01393, 2018. 6
- [42] C. Yao, X. Bai, W. Liu, Y. Ma, and Z. Tu. Detecting texts of arbitrary orientations in natural images. In *2012 IEEE Conference on Computer Vision and Pattern Recognition*, pages 1083–1090, June 2012. 5
- [43] C. Yao, X. Bai, N. Sang, X. Zhou, S. Zhou, and Z. Cao. Scene text detection via holistic, multi-channel prediction. *CoRR*, abs/1606.09002, 2016. 1, 2
- [44] C. Zhang, B. Liang, Z. Huang, M. En, J. Han, E. Ding, and X. Ding. Look more than once: An accurate detector for text of arbitrary shapes. *CoRR*, abs/1904.06535, 2019. 1, 2, 5, 6
- [45] Z. Zhang, C. Zhang, W. Shen, C. Yao, W. Liu, and X. Bai. Multi-oriented text detection with fully convolutional networks. *CoRR*, abs/1604.04018, 2016. 1, 2, 7
- [46] X. Zhou, C. Yao, H. Wen, Y. Wang, S. Zhou, W. He, and J. Liang. East: An efficient and accurate scene text detector. In *The IEEE Conference on Computer Vision and Pattern Recognition (CVPR)*, July 2017. 1, 2, 3, 7
- [47] Y. Zhu and J. Du. Textmountain: Accurate scene text detection via instance segmentation. *CoRR*, abs/1811.12786, 2018. 2